

# High-Performance Micro-Transfer-Printed Silicon Photonic DBR Laser

Aaron Zilkie<sup>(1)</sup>, Ludovic Caro<sup>(1)</sup>, Mohamad Dernika<sup>(1)</sup>, Alison Perrott<sup>(1)</sup>, Dhiraj Kumar<sup>(1)</sup>, Iain Anteney<sup>(1)</sup>  
Guomin Yu<sup>(1)</sup>, Hua Yang<sup>(1)</sup>

<sup>(1)</sup> Rockley Photonics, [aaron.zilkie@rockleyphotonics.com](mailto:aaron.zilkie@rockleyphotonics.com)

**Abstract** We report a silicon photonics DBR laser made with an RSOA micro transfer printed into a multi-micron silicon photonic circuit in an edge-coupling scheme. The high power reported represents the first micro-transfer-printed silicon photonics laser that has performance matching commercial state-of-the-art heterogeneous silicon photonics lasers.

## Introduction

Silicon photonics is a key technology to bring photonic integrated circuits (PICs) to a wide range of photonic applications because it enables the miniaturization of photonic systems by integrating key optical functions onto a single chip. However, for silicon photonics technologies to achieve the goals of broad applicability in multiple market applications and large-scale deployment, it is important to integrate III-V active devices in large number ubiquitously in the circuit, and with high integration densities. As lasers are needed in every application in photonics, an integrated III-V laser is arguably the most important component in a photonic integrated circuit. Various techniques for integration of III-V actives to silicon photonic waveguides have been demonstrated, with the techniques generally falling into two categories: either bonding unprocessed III-V materials placed above the silicon waveguide with evanescent coupling between the silicon waveguide and III-V waveguide, or attaching fully-processed III-V devices in a recess in the silicon waveguide layer and performing edge coupling. The edge coupling scheme combined with a large-mode-size Si or SiN waveguide platform is the best approach to make PICs that

work for a broad range of applications and broad optical bandwidths, and also has numerous advantages for performance, size, and manufacturability. These advantages include i) direct compact coupling between III-V and Si/SiN waveguides (no evanescent tapers or spot-size converters needed), ii) active III-V device processing in existing III-V foundries, iii) 'back-end' integration of known good and reliable III-V devices which can be tested on the III-V wafer before integration, and iv) more favorable thermals owing to a direct thermal path to the silicon substrate since the recess can be etched through the BOX layer. Highly manufacturable hybrid flip-chip bonded hybrid lasers with low coupling losses and good performance using this approach have been reported in [1].

Here we report a silicon photonic DBR laser with 60 mW output power and > 10% WPE made by micro transfer printing (MTP) an RSOA into a multi-micron silicon photonics platform with an edge coupling scheme.

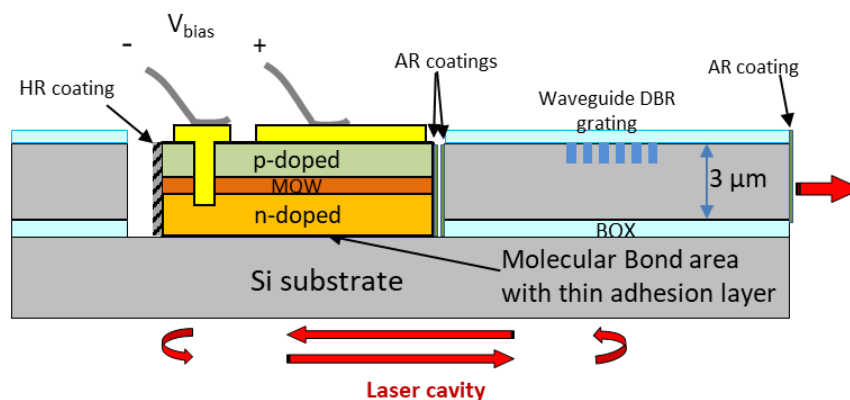


**Fig. 1:** Schematic cross-section of the heterogeneous DBR laser made with micro transfer printing in the Rockley Photonics multi-micron silicon photonics platform .

## Structure and fabrication

DBR lasers are made in the Rockley Photonics silicon photonics platform, which involves integrating III-V actives edge-coupled to a multi-micron silicon waveguide as in [1]. The general approach is to heterogeneously integrate fully processed and wafer-level-tested III-V active devices back-end-of-line in know-good-die form into recesses in the PIC using an edge-coupled scheme. The MTP DBR laser in this work is made with a reflective semiconductor optical amplifier (RSOA) micro transfer printed into a cavity etched through to the bottom of the buried oxide layer in the SOI wafer which also has a top Si layer of 3  $\mu\text{m}$ . A schematic of the cross-section of the structure is illustrated in Figure 1. Waveguides with DBR gratings are etched with deep-UV lithography into the top Si laser with a structure and reflection spectrum characteristics similar to as described in [2]. The DBR gratings were designed to have a reflection peak at a wavelength of  $\sim 1315$  nm to align to the gain peak of the RSOA. The cavities to host the MTP coupons are etched in close proximity to the DBR gratings, using a process that creates high quality vertical optical facets where the waveguides intersect the edge of the cavity. After further AR coating layer deposition and metallization, the Si wafer is spin-coated with a thin adhesive to prepare the bottom of the laser cavities for good adhesion to the laser coupons.

The epitaxial structure of the RSOA coupon is based on a standard commercial vertical p-i-n multi-quantum well (MQW) laser epi for a 1310nm wavelength laser. The thickness of the N-doped InP layer below the multiple quantum wells is designed to ensure that after bonding to the SOI cavity, the optical mode of the laser centered on the quantum wells will be vertically aligned with the SOI waveguide. Sandwiched between the N-doped InP and the substrate, a layer of AlInAs acts as sacrificial layer to facilitate the MTP release process [3,4]. The use of AlInAs allows for a high selectivity (over 1:1000 at temperatures compatible with typical industrial processing) against InP. Both P and N electrical connections are formed from the top side of the coupon. A deeply etched trench reaching the N-doped region is formed alongside the laser ridge, and P and N contacts are formed by Au metalization and patterning.

A deep etch to just above the release layer is used to create the outline of the coupon, and this etch is also used to form the front facet of the ridge waveguide, as well as the back facet. After passivation through the deposition of a dielectric layer, the back facet of the coupon is coated with metal to ensure high reflectivity.

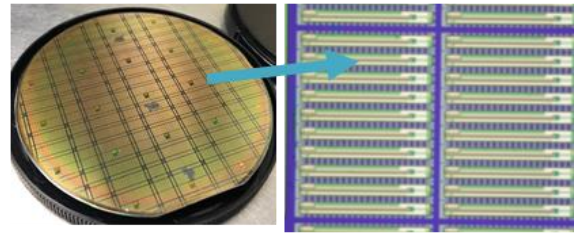


**Fig. 2:** Photograph of the fabricated 4" III-V source wafer containing RSOA coupons released and ready to be transfer printed.

Tethers are formed to keep the coupons suspended after the sacrificial layer is etched away. The tethers comprised of the photoresist used for the tether lithography, along with dielectric etched using the tether photoresist. This hybrid option allows to have safe mechanical strength of the tethers during the release process, while maintaining the option to remove the resist after release to keep only the dielectric portion of the tethers. After the tethers are defined, a selective wet etch is performed to selectively etch away the AlInAs release layer and release the coupons from the substrate. The source wafer resist is removed so that only the dielectric component of the tethers remain. This III-V MTP laser process was performed on a full 4 inch wafer in a volume III-V foundry generating  $\sim 6000$  coupons with high yield as seen in Figure 2. After descum and cleaning the source wafer is placed into the MTP tool and is ready for printing.

The MTP printing was performed by X-Celeprint using a process similar to that reported in [6-7]. The coupons are picked up from the source wafer with the stamp, moved to the target wafer where they are kept in a hover at a short distance from the target cavity. The machine vision system is used to perform the alignment of the coupon ensuring the RSOA coupon waveguide facet is aligned to the respective Si waveguide facet before the stamp and coupons are lowered down and printed onto the adhesion layer in the cavity. Accurate alignment with  $< \pm 500$  nm error is achieved by imaging optimally

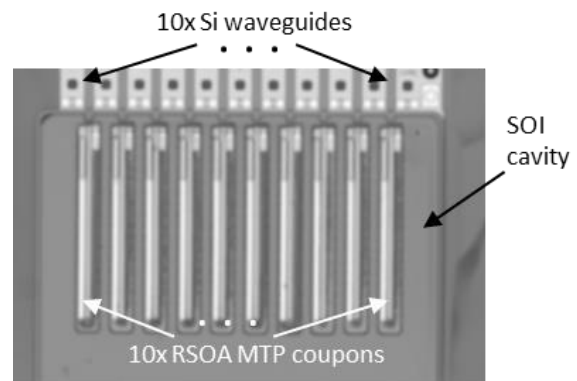


**Fig. 3:** SEM micrograph of 10 RSOA coupons transfer printed into a laser cavity in the SOI wafer.

designed fiducials on both the RSOA coupon and SOI wafer during the alignment step. The stamp is then peeled off the coupon through a mix of lateral and vertical motion, while the coupon stays in position in the cavity. Additional thermal curing of the wafer is performed to increase coupon adhesion, after which wafer-level-testing can be performed to verify the performance of each laser site and map performance yield prior to dicing and further testing. Figure 3 shows a SEM micrograph of 10 RSOA coupons printed side-by-side in one SOI cavity making an array of 10 DBR lasers.

### Experimental Results

After fabrication, the wafer was diced into chips to facilitate die-level testing of the DBR lasers. Power versus current and voltage (LIV) measurements with calibrated absolute laser output power were obtained using an integrating sphere placed in close proximity to the PIC output facet. No additional components or losses were between the DBR grating and PIC output facet so that the PIC output power is roughly equal to the laser output power in the waveguide at the output of the DBR grating. Light was also externally coupled to an optical spectrum analysis (OSA) via an SMF fiber to measure optical spectra simultaneously during an LIV measurement.

The LIV and spectra measurement results are shown in Figure 4. The laser achieved an output power of up to 60mW, and the wall-plug efficiency (WPE) efficiency measured is up to 11%. The

optical spectrum versus current in Figure 4. shows that the laser maintains single-mode operation with high SMSR throughout its full bias range. Above 26 mA an SMSR of > 40 dB was maintained at all bias current as observed on the OSA. The DBR laser threshold is measured to be 26mA and the output power rolls off above 350mA indicating good heat flow from the RSOA coupon active region directly into the Si substrate beneath [8]. The power jumps in the LIV are typical for single-mode DBR lasers of this type. To our knowledge this is the highest output power and best performance reported for a silicon photonic laser made with micro transfer printing, and the only report of one with higher than 10% WPE. Notably, by fitting the diode equation to the IV data, the series resistance of the laser is found to be  $\sim 4 \Omega$ .

### Conclusions

We have fabricated and demonstrated a high-power O-band DBR laser comprising of a III-V RSOA section MTP-bonded into a silicon PIC incorporating waveguide DBR gratings. The measured optical power of up to 60mW and 11% WPE represents the first micro-transfer-printed silicon photonics laser that has performance approaching other state-of-the-art heterogeneous silicon photonics lasers to our knowledge. The use of MTP as bonding mechanism is believed to be instrumental in achieving this performance, allowing low-loss coupling and superior thermal heat-sinking directly into the Si substrate. Furthermore, the potential for bonding throughput scalability inherent to MTP makes these devices particularly attractive for high volume product applications where a common cost and time bottleneck in the fabrication process is the bonding of III-V components onto the PIC. The optical power, SMSR, wavelength accuracy, and broad optical bandwidth facilitated by the multi-micron platform and edge-coupling scheme suggest these MTP lasers are suitable for a wide range of commercial applications from data communications to biosensing for medical wearables [9].

### Acknowledgements

The micro transfer printing was done in collaboration with X-Celeprint. The work was also collaboration with the Tyndall National Institute at University College Cork, and the Irish Photonics Integration Centre (IPIC, with funding support from the Irish government's Science Foundation Ireland (SFI) and Disruptive Technologies Innovation Fund (DTIF).

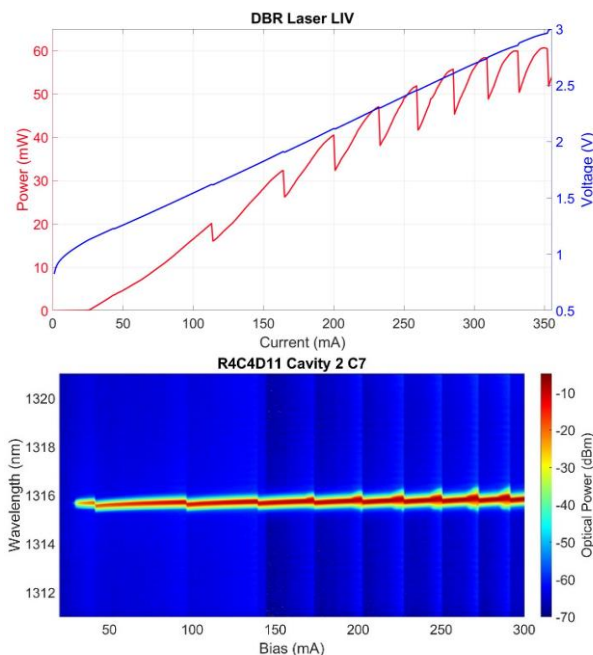


**Fig. 4:** (top) LIV curve and (bottom) spectra vs current measured from the DBR laser chip with an integrating sphere and OSA.

## References

- [1] A. J. Zilkie, P. Srinivasan, A. Trita, T. Schrans, G Yu, J. Byrd, D. A. Nelson, K. Muth, D. Lerose, M. Alalusi, K. Masuda, M. Ziebell, H. Abediasl, J. Drake, G. Miller, H. Nykanen, E. Kho, Y. Liu, H. Liang, H. Yang, F. Peters, A. Nagra, and A. G. Rickman, "Multi-micron silicon photonics platform for highly manufacturable and versatile photonic integrated circuits," *IEEE Journal of Selected Topics in Quantum Electronics*, vol. 47, no. 2, pp. 1-13, 2019, DOI: 10.1109/JSTQE.2019.2911432
- [2] A. J. Zilkie, P. Seddighian, B. J. Bijlani, W. Qian, D. C. Lee, S. Fathololoum, J. Fong, R. Shafiiha, D. Feng, B. J. Luff, X. Zheng, J. E. Cunningham, A. V. Krishnamoorthy and M. Asghari, "Power-efficient III-V/Silicon external cavity DBR lasers," *Optics Express*, vol. 20, no. 12, pp. 23456-23462, 2012, DOI: [10.1364/OE.20.023456](https://doi.org/10.1364/OE.20.023456)
- [3] B. Corbett, R. Loi, W. Zhou, D. Liu, Z. Ma, "Transfer print techniques for heterogeneous integration of photonic components," *Progress in Quantum Electronics*, Vol. 52, pp 1-17, 2017, DOI: [10.1016/j.pquantelec.2017.01.001](https://doi.org/10.1016/j.pquantelec.2017.01.001)
- [4] J. O'Callaghan, R. Loi, E. E. Mura, B. Roycroft, A. J. Trindade, K. Thomas, A. Gocalinska, E. Pelucchi, J. Zhang, G. Roelkens, C. A. Bower, and B. Corbett, "Comparison of InGaAs and InAlAs sacrificial layers for release of InP-based devices," *Optical Materials Express* 7, no. 12, pp. 4408-4414, 2017. DOI: 10.1364/OME.7.004408.
- [5] M. A. Meitl, Z.-T. Zhu, V. Kumar, K.J. Lee, X. Feng, Y.Y. Huang, I. Adesida, R.G. Nuzzo, and J.A. Rogers, "Transfer Printing by Kinetic Control of Adhesion to an Elastomeric Stamp," *Nature Materials* 5, 33-38 (2006). DOI: 10.1038/nmat1532.
- [6] <https://x-celeprint.com/technology>, accessed on 5 May 2023.
- [7] D. Gomez, T. Moore, M. A. Meitl, S. Bonafede, A. Pearson, B. Raymond, T. Weeks, K. Oswald, E. Radauscher, D. Kneeburg, J. Roe, A. Fecioru, S. Kelleher, R. F. Gul, A. Ferrell, A. J. Trindade, C. A. Bower, "Manufacturing Capability of Micro-Transfer Printing," in *Proceedings Smart Systems Integration; 13th International Conference and Exhibition on Integration Issues of Miniaturized Systems*, Barcelona, Spain, 2019, pp. 1-4
- [8] R. Loi, J. O'Callaghan, B. Roycroft, Z. Quan, K. Thomas, A. Gocalinska, E. Pelucchi, A. J. Trindade, C. A. Bower, and B. Corbett, "Thermal Analysis of InP Lasers Transfer Printed to Silicon Photonics Substrates," *Journal of Lightwave Technology* 36, no. 24, pp. 5935-5941, 2018. DOI: 10.1109/JLT.2018.2881179.
- [9] <https://rockleyphotonics.com/bioptx-band/>, accessed on 5 May, 2023